J. Fluid Mech. (1987), *vol.* 181, *pp.* 213–232
Printed in Great Britain

Finite-amplitude alternate bars

By M. COLOMBINI, G. SEMINARA AND M. TUBINO
Istituto di Idraulica, Facoltà di Ingegneria, Genova, Italy

(Received 7 July 1986 and in revised form 15 December 1986)

Following ideas developed in the field of hydrodynamic stability of laminar flows (Stuart 1971) a predictive theory is proposed to determine the development of finite-amplitude alternate bars in straight channels with erodible bottoms. It is shown that an 'equilibrium amplitude' of bedforms is reached as $t \rightarrow \infty$ within a wide range of values of the parameter $(\beta - \beta_c)/\beta_c$, where t is the time, β is the width ratio of the channel and β_c is its 'critical' value below which bars would not form. The theory leads to relationships for the maximum height and the maximum scour of bars which compare satisfactorily with the experimental data of various authors. Moreover the experimentally detected tendency of the bed perturbation to form diagonal fronts is qualitatively reproduced.

1. Introduction

River flow provides a fascinating phenomenon where the interaction between the fluid and its container determines the shape of the latter. This is mostly due to the non-cohesive character of river beds and banks though some interaction does also occur when river boundaries are cohesive. We restrict our attention to the case of non-cohesive boundaries, which exhibits an extraordinary variety of forms. In fact depending on sediment and flow parameters the flow–bottom interaction in straight channels may occur on a microscale (of the order of sediment size) leading to 'rippled' beds, or on a macroscale (of the order of flow depth) leading to the formation of 'dunes' or 'antidunes', or finally on a megascale (of the order of channel width) which gives rise to the development of 'bars'. Various other modes of interaction may occur including that associated with bank erosion leading to variation of channel alignment (meandering).

Each of the above processes can be explained in terms of an instability mechanism whereby under suitable circumstances flow in a straight channel with a flat erodible bottom loses stability to a perturbed configuration characterized by disturbances of different spatial scales. It is well known from experiments that these disturbances have a propagating character and grow until they reach an 'equilibrium amplitude'. In the last few decades a large number of studies have been devoted to the understanding of the above mechanism and to predicting the conditions for the formation of bed and channel forms. These studies were mostly linear stability theories of turbulent flow in straight channels with erodible boundaries.

Though the theoretical treatment is complicated by the turbulent character of the flow field, the above studies were largely successful in that they were able to ascertain the physical mechanisms underlying the growth of perturbations of each of the above classes: ripples, dunes and antidunes (Kennedy 1963; Engelund 1970; Hayashi 1970; Richards 1980; Sumer & Bakioglu 1984); alternate and central bars (Hansen 1967; Callander 1969; Engelund & Skovgaard 1973; Parker 1976; Fredsøe 1978); and meandering (Ikeda, Parker & Sawai 1981; Kitanidis & Kennedy 1984; Blondeaux & Seminara 1985).

Thus, even though some results are far from being conclusive, one can safely state that the body of knowledge accumulated on the linear aspects of these problems allows one to predict in gross terms: the growth rate of perturbations within the linear regime; the marginal stability conditions in the space of flow and sediment parameters; the wavelength and wave speed of perturbations selected, i.e. those corresponding to maximum growth rate.

We should point out that the works on bar stability by Parker (1976) and Fredsøe (1978) among some others were based on two-dimensional models of the flow field.

However, concerning the fundamental problem of predicting an 'equilibrium amplitude' for bedforms the available literature reduces to the nonlinear kinematic analysis by Exner (1925) and to the more recent attempt by Fredsøe (1982) referring to stationary dunes. In fact the problem of evaluating finite-amplitude effects on bedform development is generally made extremely difficult by the presence of flow separation with consequent difficulties in modelling the flow structure.

In the following we shall concentrate our attention on the nonlinear development of alternate bars. The developed structure of these bedforms is characterized by a sequence of riffles and pools: more precisely each bar unit is limited by two consecutive diagonal fronts (see figure 1) with a pool at the downstream face of each front along the channel banks. Linear stability analysis, mentioned above, cannot explain the longitudinal asymmetry embodied in the front which appears to be associated with nonlinear effects.

Though the problem of predicting an equilibrium amplitude for these bedforms is conceptually similar to those concerning disturbances of smaller lengthscale (ripples, dunes, etc.), it has the advantage that the effect of flow separation on alternate-bar development is rather weak. Indeed the presence of alternate bars contributes little to resistance at least for active gravel beds, as has been shown both by flume experiments (Shen 1962; Jaeggi 1984) and by field observations of streams at active flood stages (Bray 1979; Parker 1978).

This premise then encourages one to assume that an approximate representation of the flow field by means of a depth-averaged model, which is obviously unable to predict separation, might still be suitable to model the gross features of flow structure and bed topography. Such a simplification of the flow model then allows one to try to formulate a weakly nonlinear stability theory following ideas well established in the field of hydrodynamic stability of laminar flows (see for instance Stuart 1971). The perturbation parameter is the linear disturbance growth rate in a neighbourhood of the critical conditions for alternate-bar formation. The latter are defined by a critical value β_c of the width ratio of the channel for each set of flow and sediment parameters.

This procedure is found to work successfully and leads to the prediction that for $\beta > \beta_c$ the amplitude of bed perturbations does tend to reach an 'equilibrium value' that is finite and stable being the solution of a classical amplitude equation of the Landau–Stuart type. Comparison with experimental results for the amplitude of alternate bars appears to support the convergence of the present approach within a wide range of values of the parameter $(\beta-\beta_c)/\beta_c$. Furthermore, though unable to predict details of the flow structure like local separation at the pools, the analysis does predict a tendency for the formation of diagonal fronts which appears to be associated with the role of higher harmonics of the flow field.

The ability to predict the amplitude of alternate bars is also of practical importance

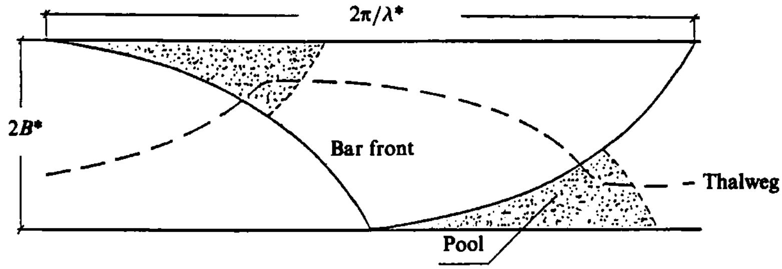

FIGURE 1. Sketch of alternate-bar structure.

since it provides the basis for preventing or controlling the processes of scouring and subsequent side-bank erosion associated with the development of these bedforms. This problem has acquired an increasing importance in highly developed countries with densely populated areas where river regulation work, such as channelization and artificial straightening motivated by land reclamation purposes, led to the unexpected appearance of alternate bars with consequent risks of bridge or bank failures (Ikeda 1982).

In §2 we formulate the problem of shallow-water flow in straight channels with erodible bottoms. In §3 we give some results of a linear stability analysis of uniform flow in straight channels with respect to disturbances of the 'bar' type; §4 is devoted to formulating and solving the weakly nonlinear stability problem posed in the neighbourhood of the critical conditions. Finally, theoretical results and comparison with experimental findings follow in §5 along with some discussion of the limits of validity of the present approach.

2. Formulation of the problem

Let us consider flow in a straight alluvial channel with constant width $2B^*$ and non-erodible banks. The channel width is assumed to be large enough for the flow to be modelled as two-dimensional.

Let s^* be the longitudinal coordinate, n^* the radial distance from the longitudinal axis and t^* the time. The St Venant equations of quasi-steady shallow-water flow in a straight channel with a slowly varying erodible bottom are written in terms of the above coordinates in the form

$$VU_{,n}+UU_{,s} = -H_{,s}-\frac{\beta\tau_s}{D}, \tag{1}$$

$$VV_{,n}+UV_{,s} = -H_{,n}-\frac{\beta\tau_n}{D}, \tag{2}$$

$$(VD)_{,n}+(UD)_{,s} = 0, \tag{3}$$

$$(F_0^2 H-D)_{,t}+Q_0(Q_{n,n}+Q_{s,s}) = 0, \tag{4}$$

$$V = Q_n = 0 \quad (n = \pm 1), \tag{5a, b}$$

where (U, V) are depth-averaged velocity components in the axial and radial directions respectively, τ_s and τ_n are bottom shear stresses, H is water-surface elevation, D is local depth, Q_s and Q_n are sediment flow rate components in the axial and radial directions and F_0 is the unperturbed Froude number.

Also, Q_0 is the ratio between the scale of sediment discharge and the flow rate and β is width ratio. We find

$$Q_0 = \frac{d_s^*\{(\rho_s/\rho-1)\,g d_s^*\}^{\frac{1}{2}}}{(1-p)\,D_0^*\,U_0^*}, \quad \beta = \frac{B^*}{D_0^*}, \tag{6a, b}$$

where ρ_s and d_s^* are density and diameter of the sediment modelled as uniform, ρ is water density, g is gravitational acceleration and p denotes sediment porosity; finally U_0^* and $D_0^*$are average speed and depth for the uniform unperturbed flow.

The variables have been made non-dimensional in the form

$$(U^*, V^*) = U_0^*(U, V), \quad (h^*, D^*) = D_0^*(F_0^2 H, D), \tag{7a, b}$$

$$(s^*, n^*) = B^*(s, n), \quad (\tau_s^*, \tau_n^*) = \rho U_0^{*2}(\tau_s, \tau_n), \tag{7c, d}$$

$$(Q_s^*, Q_n^*) = d_s^* \left\{\left(\frac{\rho_s}{\rho}-1\right) g d_s^*\right\}^{\frac{1}{2}} (Q_s, Q_n), \quad t^* = \frac{B^*}{U_0^*} t. \tag{7e, f}$$

The boundary conditions (5) express the physical requirement that the channel walls be impermeable both to the flow and to the sediment.

In order to 'close' the mathematical problem we need to formulate expressions which relate shear stresses $\boldsymbol{\tau}$ and sediment flow rate $\boldsymbol{Q}$ to flow characteristics. Following a well-established procedure (see for instance Parker 1976; or Blondeaux & Seminara 1985, hereinafter referred to as B&S) we express the shear stress $\boldsymbol{\tau}$ in terms of a friction coefficient C defined by the relationship

$$\boldsymbol{\tau} = (\tau_s, \tau_n) = (U, V)\,(U^2 + V^2)^{\frac{1}{2}}\,C. \tag{8}$$

In the following we shall assume the unperturbed bed configuration to be planar and employ Einstein's (1950) formula

$$C^{-\frac{1}{2}} = 6 + 2.5 \ln\left(\frac{D}{2.5\,d_s}\right), \tag{9}$$

where the roughness parameter has been put equal to $(2.5\,d_s^*)$ after Engelund & Hansen (1967) and a non-dimensional sediment diameter $d_s = d_s^*/D_0^*$ has been introduced.

Assuming sediment to be transported mainly as bed load and modelling the influence of transverse bed slope on the direction and intensity of bed-load motion as suggested by Engelund (1981) (see also Parker 1984; and B&S) we associate the local direction of sediment transport with an average direction of particle trajectories which deviates from the direction of average shear stresses under the action of gravity. Thus in non-dimensional form we write

$$\boldsymbol{Q} = (Q_s, Q_n) = (\cos\delta, \sin\delta)\,\Phi. \tag{10}$$

For relatively small values of δ Engelund (1981) derives the following formula:

$$\sin\delta = V(U^2 + V^2)^{-\frac{1}{2}} - \frac{r}{\beta \vartheta^{\frac{1}{2}}} (F_0^2 H - D)_{,n} \tag{11}$$

where ϑ is Shields parameter and r is a constant which Engelund (1981) suggested should assume the value (0.5–0.6). In the present calculations, in accordance with Olesen's (1983) results, lower values of r (around 0.3) have been found to lead to more satisfactory predictions of alternate-bar formation compared with experimental data.

We must stress the approximated character of (11) in the present context. Indeed not only does the derivation of (11) obviously require an interpretation in a somewhat 'averaged' sense of the dynamics of sediment grains along curved paths on a sloping bottom, but it applies to a linear context. The extension of (11) to the weakly nonlinear case is possible but would involve algebraic complications which do not seem justified at this stage. Obviously further investigations are required to substantiate the implication of neglecting this effect.

Finally the equilibrium sediment load function Φ is expressed employing the Meyer Peter–Muller formula in the form given by Chien (1954), namely

$$\Phi = 8(\vartheta - \vartheta_{\mathrm{cr}})^{\frac{3}{2}}, \quad \vartheta_{\mathrm{cr}} = 0.047. \qquad (12a, b)$$

We point out that the case where the 'undisturbed' bed is dune covered has not been considered: indeed, as suggested by one of the referees, alternate bars are found to coexist with dunes only in sandy rivers. The analysis of this case is not obvious, possibly requiring a more accurate three-dimensional model of the flow field, separation being a crucial feature of the flow structure characteristic of dunes. Furthermore the distinct role of sediment transported in suspension might be relevant at least for large values of ϑ.

3. Linear theory

Linear theory investigates the conditions required for the unperturbed uniform flow to lose stability to perturbations periodic in the s-direction and small enough for linearization to be a valid approximation. Thus let us examine disturbed flows of the form

$$(U, D, H, V) = (1, 1, H_0, 0) + A(U_1, D_1, H_1, V_1), \qquad (13)$$

$$(\tau_s, \tau_n, Q_s, Q_n) = (C_0, 0, \Phi_0, 0) + A(\tau_{s1}, \tau_{n1}, Q_{s1}, Q_{n1}), \qquad (14)$$

with A small (strictly infinitesimal). In (14) C_0 and Φ_0 respectively denote the friction coefficient and bed-load function of the undisturbed uniform flow.

On substituting from (13) and (14) into the differential system (1)–(4) and performing the linearization, the following differential problem is obtained:

$$U_{1,s} + H_{1,s} + \beta(\tau_{s1} - D_1 C_0) = 0, \qquad (15a)$$

$$V_{1,s} + H_{1,n} + \beta\tau_{n1} = 0, \qquad (15b)$$

$$U_{1,s} + V_{1,n} + D_{1,s} = 0, \qquad (15c)$$

$$F_0^2 H_{1,t} - D_{1,t} + Q_0(Q_{n1,n} + Q_{s1,s}) = 0, \qquad (15d)$$

where, using the relationships (8)–(12), τ_{s1}, τ_{n1}, Q_{s1} and Q_{n1} can be expressed in the form

$$\tau_{s1} = C_0(s_1 U_1 + s_2 D_1), \quad \tau_{n1} = C_0 V_1, \qquad (16a, b)$$

$$Q_{s1} = \Phi_0(f_1 U_1 + f_2 D_1), \quad Q_{n1} = \Phi_0\{V_1 - R(F_0^2 H_{1,n} - D_{1,n})\}, \qquad (16c, d)$$

with

$$s_1 = 2(1 - C_T)^{-1}, \quad s_2 = C_D(1 - C_T)^{-1}, \qquad (17a, b)$$

$$f_1 = \frac{2\Phi_T}{1 - C_T}, \quad f_2 = \Phi_D + \frac{C_D \Phi_T}{1 - C_T}, \quad R = \frac{r}{\beta\vartheta_0^{\frac{1}{2}}}, \qquad (17c\text{–}e)$$

where ϑ_0 is Shields parameter of the undisturbed uniform flow, and C_D, C_T, Φ_D and Φ_T are defined as

$$C_D = \frac{1}{C_0}\frac{\partial C}{\partial D}, \quad C_T = \frac{\vartheta_0}{C_0}\frac{\partial C}{\partial \vartheta}, \quad \Phi_D = \frac{1}{\Phi_0}\frac{\partial \Phi}{\partial D}, \quad \Phi_T = \frac{\vartheta_0}{\Phi_0}\frac{\partial \Phi}{\partial \vartheta}. \qquad (18a\text{–}d)$$

A normal mode analysis of the perturbation is then performed by assuming

$$(U_1, D_1, H_1, V_1) = \exp(\Omega t)\,(S_m(n)\,u_1, S_m(n)\,d_1, S_m(n)\,h_1, C_m(n)\,v_1)\,E_1(s,t)+\text{c.c.} \quad (m \text{ odd}), \quad (19a)$$

$$(U_1, D_1, H_1, V_1) = \exp(\Omega t)\,(C_m(n)\,u_1, C_m(n)\,d_1, C_m(n)\,h_1, S_m(n)\,v_1)\,E_1(s,t)+\text{c.c.} \quad (m \text{ even}), \quad (19b)$$

where c.c. (or an overbar) denotes the complex conjugate of a complex number and we define

$$S_m(n) = \sin(\tfrac{1}{2}\pi mn), \quad C_m(n) = \cos(\tfrac{1}{2}\pi mn), \qquad (20a, b)$$

$$E_m = \exp m\mathrm{i}(\lambda s - \omega t), \qquad (20c)$$

with λ, ω and Ω real quantities that denote wavenumber, angular frequency and growth rate of the perturbation respectively.

On substituting from (19) and (20) into (15) and (16) the differential system (15) is transformed into the following linear homogeneous algebraic system:

$$a_{i1}u_1 + a_{i2}v_1 + a_{i3}h_1 + a_{i4}d_1 = 0 \quad (i = 1,2,3,4), \qquad (21)$$

where, for the case of alternate bars ($m = 1$)

$$a_{11} = \mathrm{i}\lambda + \beta C_0 s_1, \quad a_{12} = a_{21} = a_{24} = a_{33} = 0, \qquad (22a\text{–}e)$$

$$a_{13} = a_{31} = a_{34} = \mathrm{i}\lambda, \quad a_{14} = \beta C_0(s_2 - 1), \qquad (22f\text{–}i)$$

$$a_{22} = \mathrm{i}\lambda + \beta C_0, \quad a_{23} = -a_{32} = \tfrac{1}{2}\pi, \qquad (22j\text{–}l)$$

$$a_{41} = \mathrm{i}\lambda Q_0 \Phi_0 f_1, \quad a_{42} = -\tfrac{1}{2}Q_0 \Phi_0 \pi, \qquad (22m, n)$$

$$a_{43} = F_0^2(\tfrac{1}{4}Q_0 \Phi_0 R\pi^2 + \Omega - \mathrm{i}\omega), \qquad (22o)$$

$$a_{44} = Q_0 \Phi_0(\mathrm{i}\lambda f_2 - \tfrac{1}{4}\pi^2 R) - \Omega + \mathrm{i}\omega. \qquad (22p)$$

The algebraic eigenrelation associated with the system (21) defines a dispersion relation which takes the form of (50) of B&S, and can be written in the general form

$$f(\Omega, \omega, \lambda, \beta; \vartheta, d_s) = 0. \qquad (23)$$

For given values of ϑ and d_s (23) allows one to define 'neutral' conditions by requiring that the amplification factor Ω of the bar perturbation should vanish. In the plane (λ, β) this condition determines a neutral curve which may exhibit a minimum at $\lambda = \lambda_c$ and $\beta = \beta_c$. A typical neutral curve is plotted in figure 2 for the case of alternate bars ($m = 1$).

However before investigating nonlinear effects it may help the reader to point out that a simple physical interpretation of bar instability can be given following the line of reasoning proposed by Engelund & Fredsøe (1982) to explain the development of mesoforms. In fact, if the linear solution is written in the form

$$\begin{bmatrix} F_0^2 H_1 - D_1 \\ H_1 \\ Q_{s1} \end{bmatrix} = \begin{bmatrix} \eta_r \\ H_r \\ Q_{sr} \end{bmatrix} \exp(\Omega t)\sin(\tfrac{1}{2}mn\pi) \begin{bmatrix} \cos(\lambda s - \omega t) \\ \cos(\lambda s - \omega t - \delta_1) \\ \cos(\lambda s - \omega t - \delta_2) \end{bmatrix} \qquad \begin{matrix} (24a) \\ (24b) \\ (24c) \end{matrix}$$

$$Q_{n1} = Q_{nr}\exp(\Omega t)\cos(\tfrac{1}{2}mn\pi)\cos(\lambda s - \omega t - \delta_3), \qquad (24d)$$

sediment continuity leads to the following relationship for the growth rate Ω:

$$\frac{\Omega}{Q_0} = -\left(\frac{\lambda Q_{sr}}{\eta_r}\right)\sin(\delta_2) + \left(\frac{\pi m Q_{nr}}{2\eta_r}\right)\cos(\delta_3). \qquad (25)$$

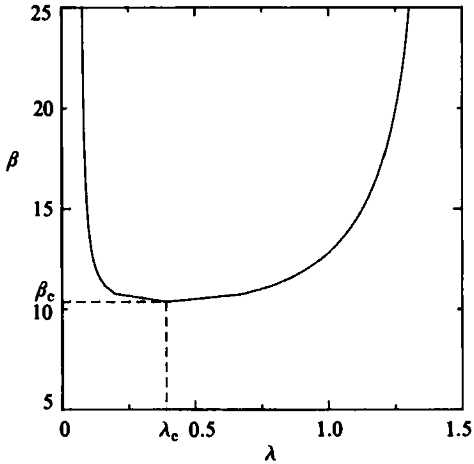

FIGURE 2. A typical neutral curve for alternate-bar formation ($\vartheta = 0.3, d_s = 0.01$, unperturbed bed assumed to be plane).

Thus instability is shown to depend not only on the phase lag δ_2 between bed profile and longitudinal sediment transport, as in the case of two-dimensional mesoforms, but also on the phase lag δ_3 between bed profile and transverse sediment transport. A discussion similar to that given by Engelund & Fredsøe (1982) suggests that the contribution of fluid friction to δ_2 is negative (i.e. destabilizing) and dominant when sediment transport mainly occurs as bed load.

The contribution of transverse sediment transport to Ω consists of two terms. The former is proportional to transverse shear stress, i.e. to V_1. The transverse component of the momentum equation (15*b*), along with (16*b*), suggests that V_1 lags behind H_1, the phase lag ranging between π and $\frac{3}{2}\pi$. Since H_1 is nearly in opposition with respect to bed profile ($\delta_1 \simeq \pm\pi$), it follows that the first contribution to δ_3 ranges between $-\frac{1}{2}\pi$ and 0, leading to a contribution for Ω that is positive. It may also be readily seen to be proportional to m, thus predicting increasing instability for higher-order modes.

The second contribution of transverse sediment transport to Ω is related to the effect of gravity which is obviously stabilizing and proportional to m^2 (see (15*d*), (16*d*) or the dispersion relation given by B&S, equation 50). The latter effect inhibits the development of higher-order modes and its balance with the destabilizing effects previously discussed determines the number of branches (m) selected by the instability process and the wavenumber associated with maximum growth.

Within the context of a linear theory the amplitude A is an arbitrary infinestimal factor. In the next section we shall relax the linear constraint by assuming that β and λ fall within the neighbourhood of the critical conditions.

4. Weakly nonlinear theory

We seek a finite-amplitude solution, restricting our attention to the weakly nonlinear regime defined by the conditions

$$\beta = \beta_c(1+\epsilon), \quad \lambda = \lambda_c + \lambda_1 \epsilon. \tag{26a, b}$$

In (26*a*, *b*) it is assumed that $\epsilon \ll 1$, though it will appear in the following that the present approach is surprisingly convergent even for $\epsilon \sim O(1)$.

It may be useful to clearly point out the kind of experiment implied by the assumption (26*a*). We consider a given uniform flow per unit width (i.e. we assume the basic water-surface slope S, the basic uniform flow depth D_0^* and the basic discharge per unit width to be given) and allow the width of the channel to vary in the neighbourhood of the critical value below which alternate bars would not develop according to the linear theory. Furthermore (26*b*) implies that disturbances are followed in the weakly nonlinear regime allowing their wavenumber λ to be 'slightly' perturbed with respect to the critical value λ_c.

Following the lead of Stuart (1971) we employ a multiple-scale technique and define a 'slow' timescale T associated with the growth of perturbations such that

$$T = \epsilon t, \quad \frac{\partial}{\partial t} \rightarrow \frac{\partial}{\partial t} + \epsilon \frac{\partial}{\partial T}. \tag{27a, b}$$

In order to derive the order of magnitude of the amplitude of perturbations we follow the usual argument of hydrodynamic stability: nonlinearity gives rise to interactions between the fundamental and itself which lead to the generation of higher harmonics both in the longitudinal and in the transverse directions. Following the above cascade process one finds that the fundamental (19) is reproduced at third order, which leads to the generation of secular terms. In order to prevent their occurrence the 'slow' time dependence of the amplitude of the fundamental must also be forced to produce a contribution at third order.

In other words $\epsilon\, \partial A/\partial T$ must balance A^3, which occurs provided $A \sim O(\epsilon^{\frac{1}{2}})$. We then expand the solution in the form

$$(U, D, H, V) = (1, 1, H_0, 0) + \sum_{p=1}^{3} (U_p, D_p, H_p, V_p)\,(\epsilon^{\frac{1}{2}})^p + O(\epsilon^{\frac{4}{2}}), \tag{28}$$

$$(\tau_s, \tau_n, Q_s, Q_n) = (C_0, 0, \Phi_0, 0) + \sum_{p=1}^{3} (\tau_{sp}, \tau_{np}, Q_{sp}, Q_{np})\,(\epsilon^{\frac{1}{2}})^p + O(\epsilon^{\frac{4}{2}}). \tag{29}$$

4.1. $O(\epsilon^{\frac{1}{2}})$

On substituting from (28), (29) into the differential system (1)–(4) and equating like powers of ϵ, at $O(\epsilon^{\frac{1}{2}})$ we obtain the differential problem (15*a–d*) with β replaced by β_c. This system admits a solution of the form

$$(U_1, D_1, H_1, V_1) = A(T)\,\{S_1(n)\,u_1, S_1(n)\,d_1, S_1(n)\,h_1, C_1(n)\,v_1\}\,E_1(s,t) + \text{c.c.}, \tag{30}$$

where (u_1, d_1, h_1, v_1) are solutions of the algebraic system (21) with m equal to 1, (λ, β, ω) again replaced by $(\lambda_c, \beta_c, \omega_c)$ and Ω vanishing. For the sake of convenience the latter will be written in the form

$$\mathrm{L}_{11} \begin{bmatrix} u_1 \\ v_1 \\ h_1 \\ d_1 \end{bmatrix} = 0, \tag{31}$$

with L_{11} an algebraic operator with an obvious definition. The function $A(T)$ in (30) is now a 'slowly varying' function of time to be determined. Obviously in the linear regime (i.e. for $T \rightarrow -\infty$) A will have to exhibit an exponential behaviour.

4.2. $O(\epsilon)$

The next-order problem is obtained by substituting from (28), (29) into (1)–(5) and equating terms $O(\epsilon)$. We find

$$U_{2,s}+H_{2,s}+\beta_c(\tau_{s2}-C_0 D_2) = -U_1 U_{1,s}-V_1 U_{1,n}-\beta_c(C_0-\tau_{s1}D_1+C_0 D_1^2), \quad (32a)$$

$$V_{2,s}+H_{2,n}+\beta_c \tau_{n2} = -V_1 V_{1,n}-U_1 V_{1,s}+\beta_c D_1 \tau_{n1}, \quad (32b)$$

$$U_{2,s}+V_{2,n}+D_{2,s} = -D_1 V_{1,n}-V_1 D_{1,n}-U_1 D_{1,s}-D_1 U_{1,s}, \quad (32c)$$

$$F_0^2 H_{2,t}-D_{2,t}+Q_0(Q_{n2,n}+Q_{s2,s}) = 0. \quad (32d)$$

Again in order to transform the system (32*a–d*) into a differential problem for (U_2, D_2, H_2, V_2) one needs to express τ_{s2}, τ_{n2}, Q_{n2} and Q_{s2} in terms of the above variables using the 'constitutive' relationships already mentioned. This procedure is straightforward but involves a considerable amount of algebra. We eventually find

$$\tau_{s2} = C_0\{[A^2E_2(C_2(n)\,t_{s22}+t_{s02})+\text{c.c.}]+A\bar{A}(C_2(n)\,t_{s20}+t_{s00})\}, \quad (33a)$$

$$Q_{s2} = \Phi_0\{[A^2E_2(C_2(n)\,q_{s22}+q_{s02})+\text{c.c.}]+A\bar{A}(C_2(n)\,q_{s20}+q_{s00})\}, \quad (33b)$$

$$\tau_{n2} = C_0\{(A^2E_2\,S_2(n)\,t_{n22}+\text{c.c.})+A\bar{A}S_2(n)\,t_{n20}\}, \quad (33c)$$

$$Q_{n2} = \Phi_0\{(A^2E_2\,S_2(n)\,q_{n22}+\text{c.c.})+A\bar{A}S_2(n)\,q_{n20}\}. \quad (33d)$$

In each of the coefficients of (33*a–d*) two components can be distinguished, the former involving linear expressions in terms of the $O(\epsilon)$-components of the flow field, the latter involving products of the $O(\epsilon^{\frac{1}{2}})$-components. Thus we write

$$(t_{s20}, t_{s22}, t_{s00}, t_{s02}) = (t'_{s20}, t'_{s22}, t'_{s00}, t'_{s02})+s_1(u_{20}, u_{22}, u_{00}, u_{02})+s_2(d_{20}, d_{22}, d_{00}, d_{02}), \quad (34a)$$

$$(q_{s20}, q_{s22}, q_{s00}, q_{s02}) = (q'_{s20}, q'_{s22}, q'_{s00}, q'_{s02})+f_1(u_{20}, u_{22}, u_{00}, u_{02})+f_2(d_{20}, d_{22}, d_{00}, d_{02}), \quad (34b)$$

$$(t_{n20}, t_{n22}) = (t'_{n20}, t'_{n22})+(v_{20}, v_{22}), \quad (34c)$$

$$(q_{n20}, q_{n22}) = (q'_{n20}, q'_{n22})+(v_{20}, v_{22})+R\pi\{F_0^2(h_{20}, h_{22})-(d_{20}, d_{22})\}, \quad (34d)$$

with the primed coefficients given explicitly in Appendix A. For simplicity the functions $t_{n02}, t_{n00}, q_{n02}, q_{n00}$ are not included in (34*c, d*) because they are seen to vanish owing to the sidewall boundary condition expressed below.

In (34*a–d*) the following decomposition of the $O(\epsilon)$ solution has been assumed:

$$(U_2, D_2, H_2) = \{A^2E_2[C_2(n)\,(u_{22}, d_{22}, h_{22})+(u_{02}, d_{02}, h_{02})]+\text{c.c.}\}$$
$$+A\bar{A}\{C_2(n)\,(u_{20}, d_{20}, h_{20})+(u_{00}, d_{00}, h_{00})\}+(0, 0, H_{00}), \quad (35a)$$

$$V_2 = \{A^2E_2(S_2(n)\,v_{22}+v_{02})+\text{c.c.}\}+A\bar{A}(S_2(n)\,v_{20}+v_{00}). \quad (35b)$$

It appears from (35*a*) that the nonlinear iteractions produce at $O(\epsilon)$ a correction (u_{00}, d_{00}, h_{00}) of the basic uniform flow.

Furthermore a correction $H_{00,s}$ is required for the basic water-surface slope since the actual width ratio has been expressed in the form (26*a*); thus

$$H_{00,s} = -\beta_c C_0. \quad (36)$$

Clearly the above correction is due to the non-dimensionalization employed where different lengthscales have been used for h^* and s^*.

On substituting from (33) and (35) into (32), after some manipulations we then find the following linear non-homogeneous systems.

The system for the harmonic of order 2 in the transverse direction and order 0 in the longitudinal direction is

$$\mathrm{L}_{20}\begin{bmatrix} u_{20} \\ v_{20} \\ h_{20} \\ d_{20} \end{bmatrix} + \begin{bmatrix} \{\frac{1}{4}\pi(u_1\bar{v}_1)+\frac{1}{2}\beta_c C_0(d_1\bar{t}_{s1}-d_1\bar{d}_1)+\mathrm{c.c.}\}+\beta_c C_0 t'_{s20} \\ \bar{v}_1\frac{1}{2}\{-\frac{1}{2}\pi v_1 - \mathrm{i}\lambda_c u_1+\beta_c C_0(t_{s1}-u_1-d_1)\}+\mathrm{c.c.} \\ \frac{1}{2}\pi d_1\bar{v}_1+\mathrm{c.c.} \\ Q_0\Phi_0\frac{1}{2}\{-\pi v_1\bar{u}_1+\frac{1}{4}R\pi^2\bar{t}_{s1}(F_0^2h_1-d_1) \\ \quad +\pi\bar{q}_{s1}[v_1-\frac{1}{2}R\pi(F_0^2h_1-d_1)]\}+\mathrm{c.c.} \end{bmatrix} = 0, \tag{37}$$

where t_{s1} and q_{s1} are the coefficients of the expansions of (τ_{s1}/C_0), (Q_{s1}/Φ_0) in the form (30) and L_{pq} is the operator obtained from L_{11} by replacing $\mathrm{i}(\lambda_c, \omega_c)$ with $q\mathrm{i}(\lambda_c, \omega_c)$ and $\frac{1}{2}\pi$ with $[(-1)^{p-1}\frac{1}{2}p\pi]$.

Similarly the system for the harmonic of order 2 both in the longitudinal and transverse directions is

$$\mathrm{L}_{22}\begin{bmatrix} u_{22} \\ v_{22} \\ h_{22} \\ d_{22} \end{bmatrix} + \begin{bmatrix} \frac{1}{4}\{\pi u_1 v_1 - 2\mathrm{i}\lambda_c u_1^2+2\beta_c C_0\,(d_1 t_{s1}-d_1^2+2t'_{s22})\} \\ \frac{1}{2}v_1\{-\frac{1}{2}\pi v_1+\mathrm{i}\lambda_c u_1+\beta_c C_0(t_{s1}-u_1-d_1)\} \\ (\frac{1}{2}\pi v_1-\mathrm{i}\lambda_c u_1)d_1 \\ \frac{1}{2}Q_0\Phi_0\{-\pi v_1 u_1+\frac{1}{4}R\pi^2 t_{s1}(F_0^2h_1-d_1) \\ \quad +\pi q_{s1}[v_1-\frac{1}{2}R\pi(F_0^2h_1-d_1)]+4\mathrm{i}\lambda_c q'_{s22}\} \end{bmatrix} = 0, \tag{38}$$

and the algebraic system for the harmonic 0–2 is of the form

$$\mathrm{L}_{02}\begin{bmatrix} u_{02} \\ v_{02} \\ h_{02} \\ d_{02} \end{bmatrix} + \begin{bmatrix} \frac{1}{4}\{\pi u_1 v_1+2\mathrm{i}\lambda_c u_1^2+2\beta_c C_0(d_1^2-d_1 t_{s1}+2t'_{s02})\} \\ 0 \\ \mathrm{i}\lambda_c u_1 d_1 \\ 2\mathrm{i}\lambda_c Q_0\Phi_0 q'_{s02} \end{bmatrix} = 0. \tag{39}$$

The $O(\epsilon)$ distortion of the basic flow associated with the perturbation is governed by the algebraic system

$$\mathrm{L}_{00}\begin{bmatrix} u_{00} \\ v_{00} \\ h_{00} \\ d_{00} \end{bmatrix} + \begin{bmatrix} \{\frac{1}{4}\pi u_1\bar{v}_1+\frac{1}{2}\beta_c C_0(d_1\bar{d}_1-d_1\bar{t}_{s1})+\mathrm{c.c.}\}+\beta_c C_0 t'_{s00} \\ 0 \\ 0 \\ 0 \end{bmatrix} = 0. \tag{40}$$

The above systems are supplemented by appropriate boundary and integral conditions as follows:

(i) The requirement of V_2 vanishing at the walls implies

$$v_{00} = v_{02} = 0. \tag{41a, b}$$

(ii) The condition of vanishing sediment flow rate at the walls is automatically satisfied by the present solution.

(iii) The condition that flow discharge per unit width should not be altered by the development of perturbations reads

$$\int_{-1}^{1} UD\,\mathrm{d}n = 2. \tag{42}$$

Equation (42) is satisfied at $O(\epsilon^{\frac{1}{2}})$ and leads at $O(\epsilon)$ to the following relationships:

$$2u_{00}+2d_{00}+u_1\bar{d}_1+\bar{u}_1 d_1 = 0, \tag{43}$$

$$2u_{02}+2d_{02}+u_1 d_1 = 0. \tag{44}$$

(iv) Finally the condition of constant average reach slope gives

$$\int_0^{2\pi/\lambda} \mathrm{d}s \int_{-1}^{1} (F_0^2 H - D)\,\mathrm{d}n = \text{const.} \tag{45}$$

Equation (45) is automatically satisfied at $O(\epsilon^{\frac{1}{2}})$ and requires at $O(\epsilon)$ that

$$F_0^2 h_{00} - d_{00} = 0. \tag{46}$$

4.3. $O(\epsilon^{\frac{3}{2}})$

Finally the differential problem found at $O(\epsilon^{\frac{3}{2}})$ when substituting from (28) and (29) into (1)–(5) is

$$U_{3,s}+H_{3,s}+\beta_c(\tau_{s3}-C_0 D_3) = -U_1 U_{2,s}-U_2 U_{1,s}-V_1 U_{2,n}-V_2 U_{1,n}$$
$$-\beta_c\{C_0(2D_1 D_2-D_1^3-D_1)+\tau_{s1}(1+D_1^2-D_2)-\tau_{s2} D_1\}, \tag{47a}$$

$$V_{3,s}+H_{3,n}+\beta_c \tau_{n3} = -V_2 V_{1,n}-V_1 V_{2,n}-U_1 V_{2,s}+U_2 V_{1,s}$$
$$-\beta_c\{\tau_{n1}(1+D_1^2-D_2)-D_1\tau_{n2}\}, \tag{47b}$$

$$U_{3,s}+V_{3,n}+D_{3,s} = -D_1 V_{2,n}-D_2 V_{1,n}-V_1 D_{2,n}$$
$$-V_2 D_{1,n}-D_1 U_{2,s}-D_2 U_{1,s}-U_1 D_{2,s}-U_2 D_{1,s}, \tag{47c}$$

$$(F_0^2 H_3 - D_3)_{,t}+Q_0(Q_{n3,n}+Q_{s3,s}) = -F_0^2 H_{1,T}+D_{1,T}, \tag{47d}$$

where we again need to express $(\tau_{s3}, \tau_{n3}, Q_{n3}, Q_{s3})$ in terms of the flow field. Some tedious algebra gives

$$\tau_{s3} = C_0\{E_1 S_1[A^2\bar{A}t'_{s11}+s_1 u_{11}(T)+s_2 d_{11}(T)]+\text{c.c.}\}+\text{higher harmonics}, \tag{48a}$$

$$Q_{s3} = \Phi_0\{E_1 S_1[A^2\bar{A}q'_{s11}+f_1 u_{11}(T)+f_2 d_{11}(T)]+\text{c.c.}\}+\text{higher harmonics}, \tag{48b}$$

$$\tau_{n3} = C_0\{E_1 C_1[A^2\bar{A}t'_{n11}+v_{11}(T)]+\text{c.c.}\}+\text{higher harmonics}, \tag{48c}$$

$$Q_{n3} = \Phi_0\{E_1 C_1[A^2\bar{A}q'_{n11}+AQ_{n11}-\tfrac{1}{2}R\pi(F_0^2 h_{11}(T)-d_{11}(T))]+\text{c.c.}\}+\text{higher harmonics}, \tag{48d}$$

where the term proportional to A arises as an $O(\epsilon^{\frac{3}{2}})$ correction of the gravitational contribution to $\sin\delta$ (see (11)).

In (48*a*–*d*) the primed coefficients are quantities expressed in terms of products of the leading- or second-order components of the flow field and are given in detail in Appendix B† along with the quantity Q_{n11}. Both give non-homogeneous contributions to the $O(\epsilon^{\frac{3}{2}})$ system. In (48*a*–*d*) it has already been assumed that the solution for (U_3, D_3, H_3, V_3) can be given the form

$$(U_3, D_3, H_3) = \{E_1 S_1(n)[u_{11}(T), d_{11}(T), h_{11}(T)]+\text{c.c.}\}+\text{higher harmonics}, \tag{49a}$$

$$V_3 = \{E_1 C_1(n)\, v_{11}(T)+\text{c.c.}\}+\text{higher harmonics}. \tag{49b}$$

† Copies of Appendices B and C are available from the *Journal of Fluid Mechanics* editorial office.

Thus at third order the spatial dependence of the fundamental is reproduced. The non-homogeneous algebraic system for $(u_{11}, d_{11}, h_{11}, v_{11})$ is then found by substituting from (48) and (49) into the differential system (47), giving

$$\mathrm{L}_{11}\begin{bmatrix} u_{11} \\ v_{11} \\ h_{11} \\ d_{11} \end{bmatrix} = \begin{bmatrix} A^2\overline{A}p_1 + Ap_2 \\ A^2\overline{A}p_3 + Ap_4 \\ A^2\overline{A}p_5 + Ap_6 \\ A^2\overline{A}p_7 + Ap_8 + p_9\dfrac{\mathrm{d}A}{\mathrm{d}T} \end{bmatrix}, \tag{50}$$

where the quantities p_{1-9} are lengthy algebraic expressions involving the $O(\epsilon^{\frac{1}{2}})$ and $O(\epsilon)$ components of the flow perturbations and the basic flow. They are given in detail in Appendix C†.

For the system (50) a solvability condition has to be satisfied because its homogeneous part admits a non-trivial solution. Solvability is ensured provided the following condition is satisfied

$$\begin{vmatrix} a_{11} & a_{12} & a_{13} & (A^2\overline{A}p_1 + Ap_2) \\ a_{21} & a_{22} & a_{23} & (A^2\overline{A}p_3 + Ap_4) \\ a_{31} & a_{32} & a_{33} & (A^2\overline{A}p_5 + Ap_6) \\ a_{41} & a_{42} & a_{43} & \left(A^2\overline{A}p_7 + Ap_8 + p_9\dfrac{\mathrm{d}A}{\mathrm{d}T}\right) \end{vmatrix} = 0, \tag{51}$$

which readily reduces to the following nonlinear ordinary differential equation for the amplitude function $A(T)$:

$$\frac{\mathrm{d}A}{\mathrm{d}T} + \alpha_1 A + \alpha_2 A^2\overline{A} = 0, \tag{52}$$

where α_1 and α_2 are expressed through p_1–p_9 in terms of the solution of the $O(\epsilon^{\frac{1}{2}})$ and $O(\epsilon)$ systems. Equation (52) is of the Landau–Stuart type and thus exhibits the following important features:

(i) if the cubic term is neglected one recovers the usual exponential behaviour of $A(T)$ predicted by linear theory;

(ii) nonlinear effects inhibit growth and lead to an equilibrium amplitude A_e reached as $T \rightarrow \infty$ provided the real parts of α_1 and α_2 have different signs. In fact on manipulating (52) it is found that

$$|A_e|^2 = -\frac{\mathrm{Re}\,(\alpha_1)}{\mathrm{Re}\,(\alpha_2)}; \tag{53}$$

(iii) the phase Θ of the amplitude function is also readily derived from (52) and reads

$$A_e = |A_e| \exp \mathrm{i}\Theta(T), \tag{54a}$$

$$\Theta = -\{\mathrm{Im}\,(\alpha_1) + \mathrm{Im}\,(\alpha_2)\,|A_e|^2\}\,T. \tag{54b}$$

Equation (54*b*) shows that the wave speed of alternate bars is affected by nonlinearity.

† Copies of Appendices B and C are available from the *Journal of Fluid Mechanics* editorial office.

5. Results and discussion

Even though each of the systems derived at the various orders of approximation could in principle be solved analytically, the numerical approach was found to be far more convenient. It consisted of solving the various linear algebraic systems obtained at the various orders of approximation by a classical Gauss–Jordan elimination procedure.

We first checked that the criterion for alternate-bar formation as predicted by the linear theory was indeed confirmed by experiments. We examined the experimental results of Kinoshita (1961), Ashida & Shiomi (1966), Chang, Simons & Woolhiser (1971), Sukegawa (1971), Muramoto & Fujita (1978), Ikeda (1982) and Jaeggi (1983). It may be useful to point out that in these experiments the values of the dimensional parameters flow rate Q^*, grain size d_s^* and slope S fell in the following range:

$$Q^* = (0.2\text{–}64.3)\ \mathrm{l/s}, \quad d_s^* = (0.18\text{–}4.0)\ \mathrm{mm}, \quad S = (0.44\times 10^{-3}\text{–}0.1).$$

Figure 3 shows the results of a comparison performed for each of their experiments. The line ($\beta = \beta_c$) separates the region where alternate bars are not expected to form on the basis of the present theory from the region where they are expected to form.

It appears that the agreement is quite satisfactory and few points show disagreement. Most of them are either close to ϑ_{cr} or their classification was dubious even for the author who performed the experiment. The uncertainty associated with the region close to ϑ_{cr} arises because the theoretical value of β_c falls quite rapidly close to $\vartheta = \vartheta_{cr}$ (see figure 6 below), so that a relatively small error in ϑ_{cr} leads to a relatively large error in β_c.

Though the linear aspects of the present theory do not differ from those presented in B&S it may be helpful to compare further our predicted critical wavelengths with experimental values detected by the authors mentioned above. This comparison is shown in figure 4.

We then evaluated the equilibrium amplitude $|A_e|$ defined by (53) where $\mathrm{Re}\,(\alpha_1)$ and $\mathrm{Re}\,(\alpha_2)$ were always found to have different signs. We point out that the value of λ which leads to the maximum value of $|A_e|$ for any given set of parameters is not significantly altered with respect to λ_c. In fact we find that the value of λ_1 in (26*b*) is $O(10^{-2}\text{–}10^{-1})$.

Thus we could compute the height of alternate bars at equilibrium H_{BM} defined as in Ikeda (1982) as the difference between the maximum and minimum bed elevations within a bar unit (scaled with D_0^*). Neglecting terms $O(\epsilon^{\frac{3}{2}}|A_e|^3)$ we find

$$H_{BM} = b_1\left\{\frac{\beta-\beta_c}{\beta_c}\right\}^{\frac{1}{2}} + b_2\left\{\frac{\beta-\beta_c}{\beta_c}\right\} + O(\epsilon^{\frac{3}{2}}|A_e|^3), \tag{55}$$

where $b_1(\vartheta, d_s)$ and $b_2(\vartheta, d_s)$ are complicated functions of the components of flow field at $O(\epsilon^{\frac{1}{2}})$ and $O(\epsilon)$. They are plotted in figure 5 while figure 6 shows the function $\beta_c(\vartheta, d_s)$ for some values of d_s. Figure 7 shows a comparison between the experimental values of H_{BM} ascertained by the authors mentioned above and the theoretical predictions obtained using (55). We included data such that ($|A_e|\,\epsilon^{\frac{1}{2}}$) did not exceed 0.6 in order for the $O(|A_e|^3\,\epsilon^{\frac{3}{2}})$ term neglected in (55) to be expected to be reasonably small. Since $|A_e|$ ranges about (0.2–0.3) the range of values of ϵ included in figure 7 is rather wide and it is interesting that a satisfactory agreement is found even for high values of ϵ.

Few data are sharply underestimated. This occurs in some of the cases when β is so close to β_c that a relatively small error in the theoretical prediction of β_c leads

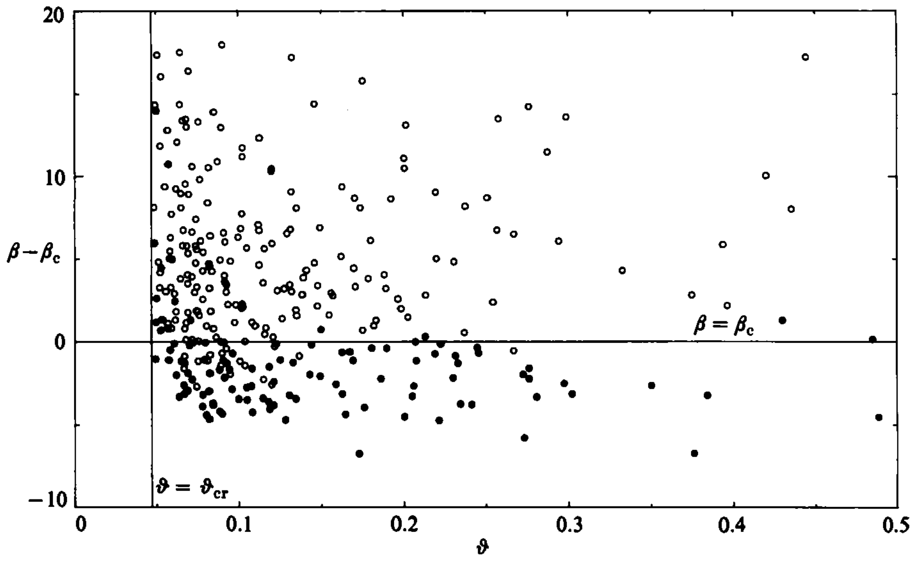

FIGURE 3. Criterion for alternate-bar formation: comparison between present results and experimental findings of various authors. Theory predicts occurrence of alternate bars if $\beta > \beta_c$ (i.e. above the solid line $\beta = \beta_c$). ○ and ● denote 'alternate bar' and 'no alternate bar' respectively as found experimentally.

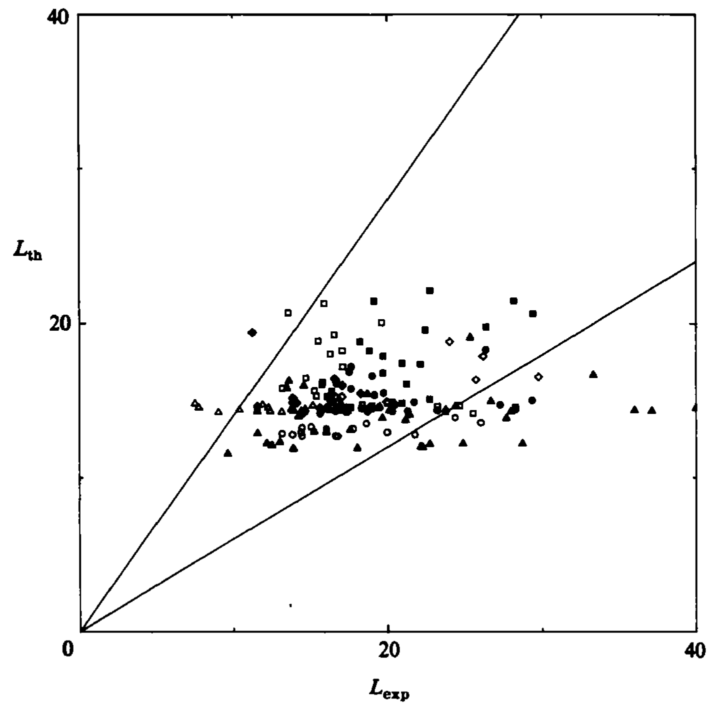

FIGURE 4. The dimensionless wavelength of alternate bars (scaled by the half width B^*) as predicted by the linear theory L_{th} is compared with experimental data L_{exp} of various authors: ○, Jaeggi (1983) PVC; ●, Jaeggi (1983) sand; □, Sukegawa (1971); ■, Kinoshita (1961)' ◇, Muramoto & Fujita (1978); ◆, Ashida & Shiomi (1966); △, Ikeda (1982); ▲, Chang, Simons & Woolhiser (1971). Data falling between solid lines are such that $|L_{th} - L_{exp}| < 40\,\%\, L_{exp}$.

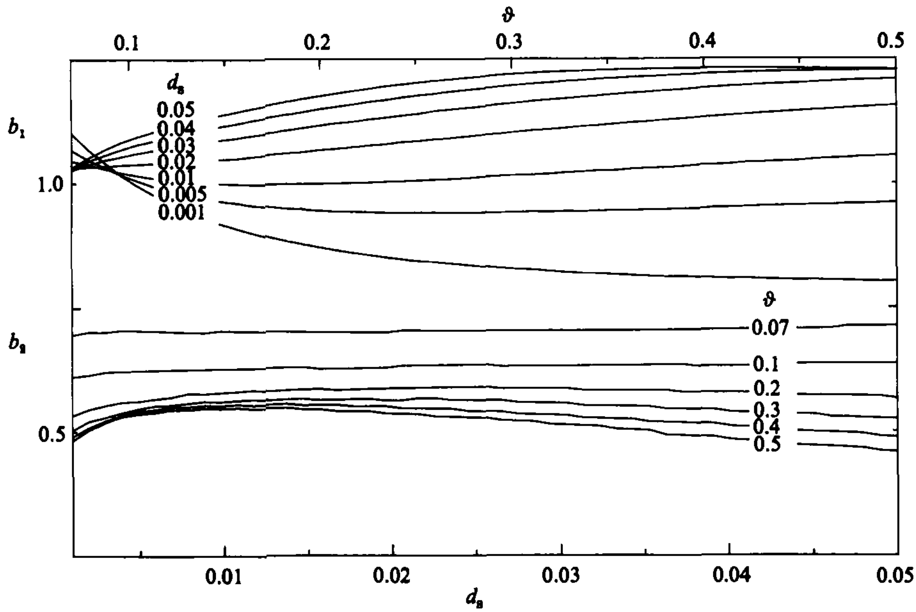

FIGURE 5. The functions b_1 and b_2 are plotted in terms of ϑ and d_s.

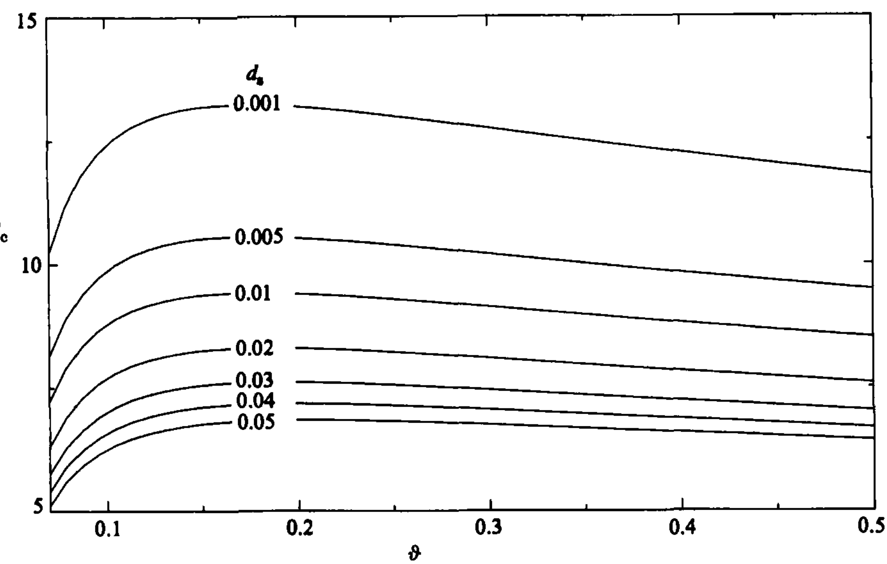

FIGURE 6. The critical value of width ratio β_c predicted by the present theory is plotted versus ϑ for some values of d_s.

to a large error in the evaluation of $(\beta-\beta_c)/\beta_c$. As mentioned above it appears from figure 6 that β_c falls quite rapidly to zero close to $\vartheta = \vartheta_{cr}$: this feature may again lead to relatively poor predictions of H_{BM} in this range.

Indeed evaluation of the percentage error associated with the comparison shows that: it is not significantly correlated with d_s; it increases slightly with increasing ϵ (i.e. with increasingly strong nonlinearity); it exhibits a sharp increase close to $\vartheta = \vartheta_{cr}$.

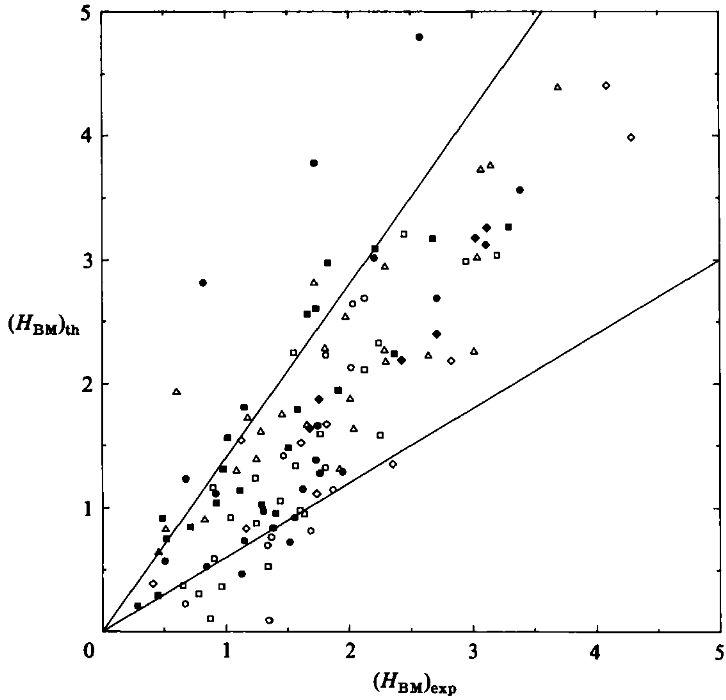

FIGURE 7. The maximum height of alternate bars as predicted by the present theory $(H_{BM})_{th}$ is compared with experimental data $(H_{BM})_{exp}$ of various authors: ○, Jaeggi (1983) PVC; ●, Jaeggi (1983) sand; □, Sukegawa (1971); ■, Kinoshita (1961); ◇, Muramoto & Fujita (1978); ◆, Ashida & Shiomi (1966); △, Ikeda (1982). Data falling between solid lines are such that $|(H_{BM})_{th}-(H_{BM})_{exp}| < 40\,\%\,(H_{BM})_{exp}$.

It may also be of some interest to compare our theoretically predicted formula (55) with the empirical formula suggested by Ikeda (1982, equations (16) and (19), pp. 36, 38) which, using the present notation, can be put in the form

$$(H_{BM})_{exp} = 0.18\, d_s^{0.45}\, \beta^{1.45}. \tag{56}$$

It appears that the influence of ϑ is ignored in (56). This seems to be a limit of the above correlation since in the neighbourhood of the critical conditions each of the quantities b_1, b_2 and β_c plotted in figures 5 and 6 are quite sensitive to variations of ϑ. Formula (56) suggests that the relative maximum height H_{BM} increases as d_s increases. Since b_1 increases with d_s for given ϑ (except for a small neighbourhood of ϑ_{cr}), b_2 is fairly independent of d_s and β_c decreases with increasing d_s for given ϑ, the qualitative trend observed by Ikeda (1982) is confirmed by our theoretical predictions.

The mean percentage error associated with the comparison plotted in figure 7 lies between $-56\,\%$ and $+28\,\%$: we point out that the present approach accounts for the presence of a ϑ-dependence for H_{BM}.

A satisfactory agreement is also found between our prediction of the maximum relative scour (η_M/H_{BM}) (around 0.57) and the value 0.5 reported by Ikeda (1982). Figure 8 confirms the latter statement.

In figure 9 we give an overall prospectic view of bed topography for Ikeda's (1982) run n. 22, obtained by truncating our expansion at $O(\epsilon)$. Though this representation must obviously be inaccurate, some of the natural features of alternate bars appear

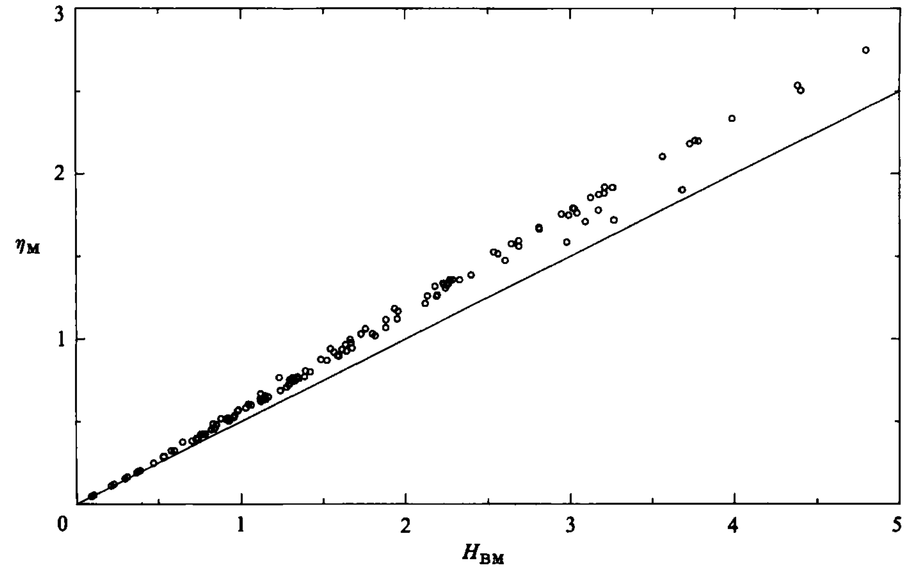

FIGURE 8. The maximum scour η_M calculated for the values of (ϑ, d_s) corresponding to the experiments referred to in figure 5 is plotted versus the maximum bar height H_{BM}. The average dependence detected by Ikeda (1982) is represented by the solid line.

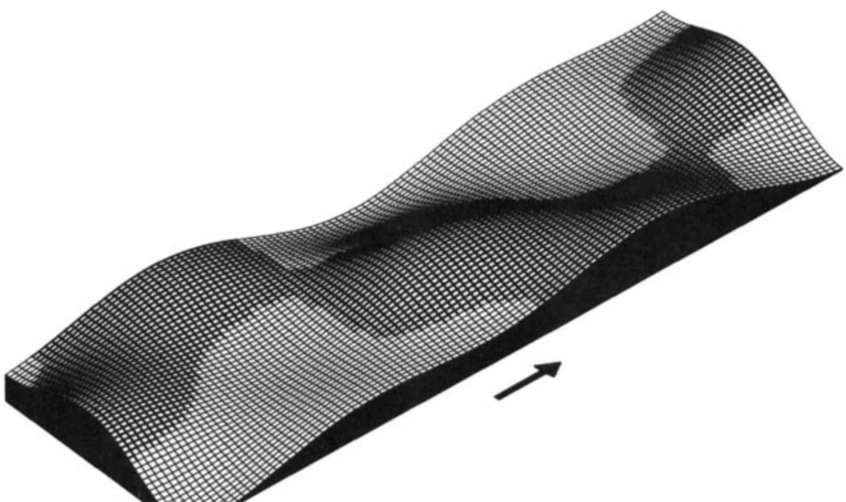

FIGURE 9. An overall prospectic view of bed topography of alternate bars as predicted by the present model accurate to $O(\epsilon)$.

to emerge, namely the formation of diagonal fronts and the increased steepness of the bottom downstream of the fronts. It may help the reader to present the values attained by the amplitudes of each second-order harmonic for the bottom elevation in the case plotted in figure 9: we find

$$|A_e|^2 (F_0^2 h_{22} - d_{22}) = (7.66 \times 10^{-3}, 0.24), \quad |A_e|^2 (F_0^2 h_{20} - d_{20}) = (0.15)$$

$$|A_e|^2 (F_0^2 h_{02} - d_{02}) = (7.81 \times 10^{-4}, 8.76 \times 10^{-4}).$$

The present theory cannot go as far as to predict separation, so that this representation is locally inadequate also owing to the limited number of harmonics retained in the computations. However the above results have shown that this limitation does not affect significantly our estimate of the height of bars.

Finally let us come to some conclusions. The model proposed appears to explain satisfactorily some physically observed features: nonlinear effects inhibit indefinite growth leading perturbations to reach an 'equilibrium amplitude'; the development of higher harmonics tends to form diagonal fronts with high downstream steepness. Also, quantitatively satisfactory predictions of the maximum height of alternate bars are possible within a surprisingly wide range of β.

However various limitations of the present analysis will need further attention. In particular a more accurate representation of the flow structure would be required, particularly under strongly nonlinear conditions ($\beta \gg \beta_c$) and further features of the natural phenomena (sediment non-uniformity, role of suspended load, etc.) should be accounted for. Finally the possible coexistence of mesoforms (dunes) and megaforms (bars) needs to be investigated.

This work was supported by MPI (Italian National Research Projects) and is also part of the junior author's (M.T.) Ph.D. thesis to be submitted to the University of Genoa.

A short preliminary version of this paper was presented at the meeting *Third International Symposium on River Sedimentation*, Jackson, 1986.

Appendix A

Coefficients of (34*a*–*d*):

$$t'_{s20} = \tfrac{1}{2}\{(s_3+s_4)(1-C_T)^{-1}\}+\text{c.c.},$$

$$t'_{s22} = \tfrac{1}{2}\{(s_5+s_6)(1-C_T)^{-1}\},$$

$$t'_{s00} = \tfrac{1}{2}\{(s_4-s_3)(1-C_T)^{-1}\}+\text{c.c.},$$

$$t'_{s02} = \tfrac{1}{2}\{(s_6-s_5)(1-C_T)^{-1}\},$$

$$q'_{s20} = \tfrac{1}{2}(f_3-f_4)+\Phi_T t'_{s20}+\text{c.c.},$$

$$q'_{s22} = \tfrac{1}{2}(f_5-f_6)+\Phi_T t'_{s22},$$

$$q'_{s00} = \tfrac{1}{2}(f_3+f_4)+\Phi_T t'_{s00}+\text{c.c.},$$

$$q'_{s02} = \tfrac{1}{2}(f_5+f_6)+\Phi_T t'_{s02},$$

$$t'_{n20} = \tfrac{1}{2}(v_1\bar{t}_{s1}-u_1\bar{v}_1)+\text{c.c.},$$

$$t'_{n22} = \tfrac{1}{2}(v_1 t_{s1}-u_1 v_1),$$

$$q'_{n20} = \tfrac{1}{8}\{-4u_1\bar{v}_1+R\pi\bar{t}_{s1}(F_0^2 h_1-d_1)+2\bar{q}_{s1}[2v_1-R\pi(F_0^2 h_1-d_1)]\}+\text{c.c.},$$

$$q'_{n22} = \tfrac{1}{8}\{-4u_1 v_1+R\pi t_{s1}(F_0^2 h_1-d_1)+2q_{s1}[2v_1-R\pi(F_0^2 h_1-d_1)]\},$$

where

$$s_3 = \tfrac{1}{2}\{6u_1\bar{u}_1-C_{DD}d_1\bar{d}_1-(4u_1+2C_{DT}d_1+C_{TT}t_{s1})\bar{t}_{s1}\},$$

$$s_4 = \tfrac{1}{2}(1+C_T)v_1\bar{v}_1,$$

$$s_5 = \tfrac{1}{2}\{6u_1^2-C_{DD}d_1^2-(4u_1+2C_{DT}d_1+C_{TT}t_{s1})t_{s1}\},$$

$$s_6 = \tfrac{1}{2}(1+C_T)\,v_1^2,$$

$$f_3 = -\tfrac{1}{8}R^2\pi^2(F_0^4 h_1 \bar{h}_1 + d_1 \bar{d}_1 - 2F_0^2 h_1 \bar{d}_1) + \tfrac{1}{2}\{R\pi(F_0^2 h_1 - d_1) + (\Phi_T - 1)\,v_1\}\,\bar{v}_1,$$

$$f_4 = \tfrac{1}{2}\{\Phi_{DD}\, d_1 \bar{d}_1 + (\Phi_{TT}\, t_{s1} + 2\Phi_{DT}\, d_1)\,\bar{t}_{s1}\},$$

$$f_5 = -\tfrac{1}{8}R^2\pi^2(F_0^2 h_1 - d_1)^2 + \tfrac{1}{2}\{R\pi(F_0^2 h_1 - d_1) + (\Phi_T - 1)\,v_1\}\,v_1,$$

$$f_6 = \tfrac{1}{2}\{\Phi_{DD}\, d_1^2 + (\Phi_{TT}\, t_{s1} + 2\Phi_{DT}\, d_1)\,t_{s1}\},$$

with

$$C_{DD} = \frac{1}{C_0}\frac{\partial^2 C}{\partial D^2}, \quad C_{TT} = \frac{\vartheta_0^2}{C_0}\frac{\partial^2 C}{\partial \vartheta^2}; \quad C_{DT} = \frac{\vartheta_0}{C_0}\frac{\partial^2 C}{\partial D\,\partial \vartheta},$$

$$\Phi_{DD} = \frac{1}{\Phi_0}\frac{\partial^2 \Phi}{\partial D^2}, \quad \Phi_{TT} = \frac{\vartheta_0^2}{\Phi_0}\frac{\partial^2 \Phi}{\partial \vartheta^2}, \quad \Phi_{DT} = \frac{\vartheta_0}{\Phi_0}\frac{\partial^2 \Phi}{\partial D\,\partial \vartheta}.$$

REFERENCES

Ashida, K. & Shiomi, Y. 1966 Study on the hydraulic behaviours of meander in channels. *Disaster Prevention Research Institute Annuals*, Kyoto Univ., No. 9, pp. 457–477.

Blondeaux, P. & Seminara, G. 1985 A unified bar–bend theory of river meanders. *J. Fluid Mech.* **157**, 449–470.

Bray, D. I. 1979 Estimating average velocity in gravel bed rivers. *Hydraul. Div., ASCE* **105** (HY9), 1103–1122.

Callander, R. A. 1969 Instability and river channels. *J. Fluid Mech.* **36**, 465–480.

Chang, H., Simons, D. B. & Woolhiser, D. A. 1971 Flume experiments on alternate bar formation. *J. Waterways, Harbors, Coastal Engng Div., ASCE* **97**, 155–165.

Chien, N. 1954 The present status of research on sediment transport. *J. Hydraul. Div., ASCE* **80**, 1954.

Einstein, H. A. 1950 The bedload function for sediment transport in open channel flow. *US Dept. Agric. Tech. Bull.* **1026**.

Engelund, F. 1970 Instability of erodible beds. *J. Fluid Mech.* **42**, 225–244.

Engelund, F. 1981 The motion of sediment particles on an inclined bed. *Tech. Univ. Denmark ISVA Prog. No.* 53, pp. 15–20.

Engelund, F. & Fredsøe, J. 1982 Sediment ripples and dunes. *Ann. Rev. Fluid Mech.* **14**, 13–37.

Engelund, F. & Hansen, E. 1967 *A Monograph on Sediment Transport in Alluvial Streams*. Copenhagen: Danish Technical Press.

Engelund, F. & Skovgaard, O. 1973 On the origin of meandering and braiding in alluvial streams. *J. Fluid Mech.* **57**, 289–302.

Exner, F. M. 1925 Uber die Wechselwirkung zwischen Wasser und Geschiebe in Flussen. *Sitzber Akad. Wiss*, pp. 165–180.

Fredsøe, J. 1978 Meadering and braiding of rivers. *J. Fluid Mech.* **84**, 609–624.

Fredsøe, J. 1982 Shape and dimensions of stationary dunes in rivers. *J. Hydraul. Div. ASCE* **108** (HY8), 932–947.

Hansen, E. 1967 On the formation of meanders as a stability problem. *Hydraulic Lab. Tech. Univ. Denmark Basic Res. Prog. Rep.*, vol. 13, pp. 9–13.

Hayashi, T. 1970 Formation of dunes and antidunes in open channels. *J. Hydraul. Div. ASCE* **96** (HY2), 357–366.

Ikeda, S. 1982 Prediction of alternate bar wavelength and height. *Rep. Dept. Found. Engng & Const. Engng, Saitama Univ.*, vol. 12, pp. 23–45.

Ikeda, S., Parker, G. & Sawai, K. 1981 Bend theory of river meanders. Part 1. Linear Development. *J. Fluid Mech.* **112**, 363–377.

Jaeggi, M. 1983 Alternierende Kiesbänke. *Mitteilungen der Versuchsanstalt für Wasserbau, Hydrologie und Glaziologie*. Zurich: E.T.H.

JAEGGI, M. 1984 Formation and effects of alternate bars. *J. Hydraul. Engng, ASCE* **110**, 142–156.

KENNEDY, J. F. 1963 The mechanics of dunes and antidunes in erodible-bed channels. *J. Fluid Mech.* **16**, 521–544.

KINOSHITA, R. 1961 Investigation of channel deformation in Ishikari River. *Rep. Bureau of Resources, Dept. Science & Technology, Japan*, pp. 1–174.

KITANIDIS, P. K. & KENNEDY, J. F. 1984 Secondary current and river meander formation. *J. Fluid Mech.* **144**, 217–229.

MURAMOTO, Y. & FUJITA, Y. 1978 The classification of meso-scale river bed configuration and the criterion of its formation. *Proc. 22nd Japanese Conf. on Hydraulics*, pp. 275–282. JSCE.

OLESEN, K. W. 1983 Alternate bars in and meandering of alluvial rivers. *Commun. Hydraul., Rep.* 7–83, Delft Univ. of Technology.

PARKER, G. 1976 On the cause and characteristic scales of meandering and braiding in rivers. *J. Fluid Mech.* **76**, 457–480.

PARKER, G. 1978 Self-formed straight rivers with equilibrium banks and mobile bed. Part 2. The gravel river. *J. Fluid Mech.* **89**, 127–147.

PARKER, G. 1984 Discussion of: Lateral bed load transport on side slopes. By S. Ikeda. *J. Hydraul. Engng, ASCE* **110**, 197–199.

RICHARDS, K. J. 1980 The formation of ripples and dunes on an erodible bed. *J. Fluid Mech.* **99**, 597–618.

SHEN, H. W. 1962 Development of bed roughness in alluvial channels. *J. Hydraul. Div. ASCE* **88** (HY3), 45–58.

STUART, J. T. 1971 Nonlinear stability theory. *Ann. Rev. Fluid Mech.* **3**, 347–370.

SUKEGAWA, N. 1971 Study on meandering of streams in straight channels. *Rep. Bureau of Resources, Dept. Science & Technology, Japan*, pp. 335–363.

SUMER, B. M. & BAKIOGLU, M. 1984 On the formation of ripples on an erodible bed. *J. Fluid Mech.* **144**, 177–190.